Perm Polytech Style: Olivenko N.A., Leshkov E.V., Zaigraev D.S., Matash V.P., Ulyanov S.M., Kudryavtsev O.A. Experimental Study of the GFRP Perforation Stochasticity Near the Ballistic Limit. *PNRPU Mechanics Bulletin,* 2025, no. 2, pp. 91-99. DOI: 10.15593/perm.mech/2025.2.08

Экспериментальное исследование стохастичности пробития стеклопластика вблизи баллистического предела / Н.А. Оливенко, Е.В. Лешков, Д.С. Заиграев, В.П. Маташ, С.М. Ульянов, О.А. Кудрявцев. – DOI: 10.15593/perm.mech/2025.2.08 // Вестник Пермского национального исследовательского политехнического университета. Механика. – 2025. – № 2. – С. 91–99.

пермский политех

ВЕСТНИК ПНИПУ. МЕХАНИКА
№ 2, 2025
PNRPU MECHANICS BULLETIN
https://ered.pstu.ru/index.php/mechanics/index



Научная статья

DOI: 10.15593/perm.mech/2025.2.08
УДК 620.171.34, 53.091

EXPERIMENTAL STUDY OF THE GFRP PERFORATION STOCHASTICITY NEAR THE BALLISTIC LIMIT

N.A. Olivenko[1], E.V. Leshkov[1], D.S. Zaigraev[2], V.P. Matash[2], S.M. Ulyanov[2], O.A. Kudryavtsev[1]

[1]South Ural State University, Chelyabinsk, Russian Federation
[2]Russian Federal Nuclear Center – Zababakhin All-Russia Research Institute of Technical Physics, Snezhinsk, Russian Federation

ARTICLE INFO

Received: 04 March 2024
Approved: 02 April 2025
Accepted for publication: 30 May 2025

Keywords:

fibre-reinforced plastic (FRP), glass fibre-reinforced plastic, high-velocity impact, ballistic limit, stochasticity, zone of mixed results, perforation frequency curve.

ABSTRACT

The work aims at experimentally analyzing features of the impact interaction of a steel spherical projectile with glass fibre-reinforced plastic (GFRP) specimens with the thicknesses of 4 mm, 6 mm, and 7.3 mm at the velocities near the corresponding ballistic limits. The experimental study was carried out in two stages. At the first stage, ballistic curves, estimations of V_{50} and limit perforation and non-perforation velocities were obtained based on the results of the first series of impact tests using the Lambert-Jonas approximation. At the second stage, a series of tests was carried out for GFRP specimens of each thickness, when the initial projectile velocity was selected so that it fell into the zone of mixed results to obtain the perforation frequency curves. Based on the results of more than 300 experiments, it was established that the perforation frequency curves for GFRP specimens with the thicknesses of 6 mm and 7.3 mm can be obtained using the normal distribution law. Also it was found that the ratio of the width of the zone of mixed results to the corresponding V_{50} estimation for two thicknesses of specimens was about 4%, which is significantly less than the scatter of the strength characteristics of GFRP specimens obtained during the static tests.

© **Nikita A. Olivenko** – Engineer, e-mail: olivenkona@susu.ru, ID: 0000-0002-9706-4056.
Egor V. Leshkov – Engineer, e-mail: leshkovev@susu.ru, ID: 0000-0001-9380-8719.
Dmitriy S. Zaigraev – Scientist, e-mail: dszaigraev@mail.ru, ID: 0009-0006-7841-1362.
Vladimir P. Matash – Laboratory Head, e-mail: matash_vladimir@mail.ru, ID: 0009-0004-1908-2410.
Sergei M. Ul'yanov – CSc in Technical Sciences, Department Head, e-mail: s.m.ulyanov@vniitf.ru, ID: 0009-0002-5018-3661.
Oleg A. Kudryavtsev – CSc in Technical Sciences, Junior Researcher of Aerospace Department, e-mail: kudriavtcevoa@susu.ru, ID: 0000-0002-8530-3128.

Оливенко Никита Алексеевич – инженер, e-mail: olivenkona@susu.ru, ID: 0000-0002-9706-4056.
Лешков Егор Валерьевич – инженер, e-mail: leshkovev@susu.ru, ID: 0000-0001-9380-8719.
Заиграев Дмитрий Сергеевич – исследователь, e-mail: dszaigraev@mail.ru, ID: 0009-0006-7841-1362.
Маташ Владимир Петрович – заведующий лабораторией, e-mail: matash_vladimir@mail.ru.
Ульянов Сергей Михайлович – к.т.н., начальник отдела, e-mail: s.m.ulyanov@vniitf.ru, ID: 0009-0002-5018-3661.
Кудрявцев Олег Александрович – к.т.н., м.н.с., e-mail: kudriavtcevoa@susu.ru, ID: 0000-0002-8530-3128.

Эта статья доступна в соответствии с условиями лицензии Creative Commons Attribution-NonCommercial 4.0 International License (CC BY-NC 4.0)
This work is licensed under a Creative Commons Attribution-NonCommercial 4.0 International License (CC BY-NC 4.0)

ЭКСПЕРИМЕНТАЛЬНОЕ ИССЛЕДОВАНИЕ СТОХАСТИЧНОСТИ ПРОБИТИЯ СТЕКЛОПЛАСТИКА ВБЛИЗИ БАЛЛИСТИЧЕСКОГО ПРЕДЕЛА

Н.А. Оливенко[1], Е.В. Лешков[1], Д.С. Заиграев[2], В.П. Маташ[2], С.М. Ульянов[2], О.А. Кудрявцев[1]

[1]Южно-Уральский государственный университет, Челябинск, Российская Федерация
[2]Российский федеральный ядерный центр – Всероссийский научно-исследовательский институт технической физики имени академика Е.И. Забабахина, Снежинск, Российская Федерация

О СТАТЬЕ

Получена: 04 марта 2024 г.
Одобрена: 02 апреля 2025 г.
Принята к публикации: 30 мая 2025 г.

Ключевые слова:

полимерный композитный материал, стеклопластик, высокоскоростной удар, баллистический предел, стохастичность, область неоднозначных результатов, кривая частости пробития.

АННОТАЦИЯ

Целью данной работы было экспериментальное исследование особенностей взаимодействия стального сферического ударника с образцами стеклопластика СТЭФ толщиной 4, 6 и 7,3 мм при скоростях вблизи соответствующих баллистических пределов. Экспериментальное исследование было проведено в два этапа. На первом этапе по результатам первой серии ударных испытаний с использованием аппроксимации Ламберта – Джонаса были построены баллистические кривые и получены оценки V_{50}, предельных скоростей пробития и непробития. На втором этапе для каждой толщины стеклопластика была проведена вторая серия испытаний, когда начальную скорость ударника подбирали таким образом, чтобы она попадала в область неоднозначных результатов с целью получения кривых частости пробития. По результатам более чем 300 испытаний было установлено, что кривые частости пробития для образцов стеклопластика толщиной 6 и 7,3 мм могут быть получены с привлечением нормального закона распределения. Также было установлено, что отношение ширины области неоднозначных результатов к соответствующей оценке V_{50} для образцов двух толщин составило около 4 %, что значительно ниже разброса прочностных характеристик образцов СТЭФ, полученных при квазистатических испытаниях.

Introduction

Fibre-reinforced plastics based on high-strength synthetic fibres are used in many industries as a structural material. In some cases, a composite structure can be subject not only to static/cyclic loading, but also to impact. Under normal operation conditions, composite structures are most often subjected to low-velocity impacts (hail, tool drop, gravel from vehicle wheels, impacts from auxiliary equipment, birds, etc.). Similar phenomena often occur during the operation of aircraft, wind generators, ship elements and bridge elements [1–4]. To provide further safe operation of composite structures, there are requirements for the residual static strength of composites in the presence of impact damages. In cases related to emergency situations, where the requirements for ensuring the integrity/tightness of the structure are imposed, the tasks of high-velocity impact interactions are also widespread [5–10]. For example, fragments formed by rotor blades fracture must be localized by the aircraft engine protective case to prevent the fuselage damage [5]. To date, a plenty of studies have been published on the experimental and computational analysis of the composite material impact loading features among which several review works [11–16] can be highlighted that quite fully reflect and structure the accumulated experience in this field.

Despite the large number of publications devoted to FRPs impact loading, there are almost no works on the random nature of the perforation process of the layered composites under high-velocity impact. When a projectile interacts with a target, there are two outcomes that indicate the target damage, and they are perforation or non-perforation (failure or resistance) [17; 18]. It is believed that at each projectile velocity V_i the target behaviour has a binary result (response) U, where U=1 if perforation takes place and U=0 if no perforation occurs. There is also a zone of mixed results (ZMR), which is characterized by two limit velocities V_0 and V_{100}. When using a probabilistic approach, V_0 determines the projectile velocity, corresponding to the zero probability of target perforation, and V_{100} determines the upper limit of the zone of mixed results and corresponds to the velocity at which the target is perforated with a 100 % probability.

When designing composite structures that can be subject to high-velocity impact, engineers are faced with the task of determining rational configurations of composite targets that would guarantee no perforation over the entire expected operating range of projectile velocities [19; 20]. In [19], using a simple protective barrier consisting of one steel plate as an example, it is presented that the solution to this problem comes down to determining the thickness of the plate for which the value V_{50} will exceed the design velocity V_D by a certain amount. Figure 1 shows the dependence of target perforation probability on the initial projectile velocity. The average value of projectile velocity in the zone of mixed results is V_{50} (the projectile velocity at which the probability of target perforation is 50 %), and the standard deviation σ characterizes the width of the zone of mixed results. Velocity V_0 is calculated based on the results of ballistic limit tests. The permissible design velocity V_D must be lower than V_0 by the design tolerance value Δ. In fact, the value of Δ is determined by the standard safety factor [19;

20]. Thus, when designing a structure, the value of the permissible velocity V_D is lower than the value V_0, then this configuration excludes the possibility of target perforation in a given operating range of projectile velocities. For simple structures consisting of, for example, a single steel plate, the width of the zone of mixed results can be quite narrow and amount to about 5 m/s. However, for more complex structures (multilayer and heterogeneous), which include structural composites, the width of ZMR can be several tens of meters per second [19].

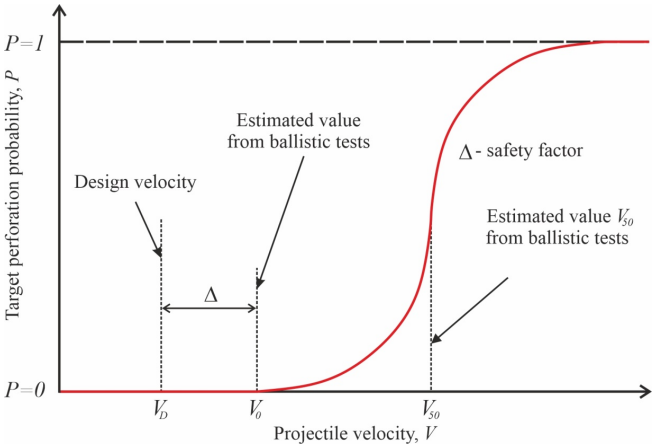


Fig. 1. Perforation probability vs projectile velocity

The works [21–27] present various approaches to processing experimental data to obtain estimates of V_0, V_{50} and V_{100}. Unfortunately, it was not possible to find in open sources any estimates of the zone of mixed results width for FRPs, as well as data on the influence of target thickness on it. Meanwhile, this information is extremely important when constructing computational models of deformation and fracture of a composite under high-velocity impact, since ballistic curves are used to verify their parameters [28].

This paper presents an experimental study on the features of the impact interaction of a steel spherical projectile with GFRP specimens with the thicknesses of 4 mm, 6 mm, and 7.3 mm at the velocities near the corresponding ballistic limits. The experimental study was carried out in two stages. At the first stage, based on the results of the first series of impact tests using the Lambert-Jonas approximation [27], ballistic curves and estimates of V_{50}, maximum perforation and non-perforation velocities were obtained for each thickness of specimens. At the second stage, another series of tests for each thickness of specimens, when the initial projectile velocity was selected so that it fell into the zone of mixed results was carried out in order to obtain perforation frequency curves. Based on the results of more than 300 impact tests, estimates of the zone of mixed results width were obtained, which can later be used by engineers and designers when creating critical structures potentially subjected to impact loading during operation.

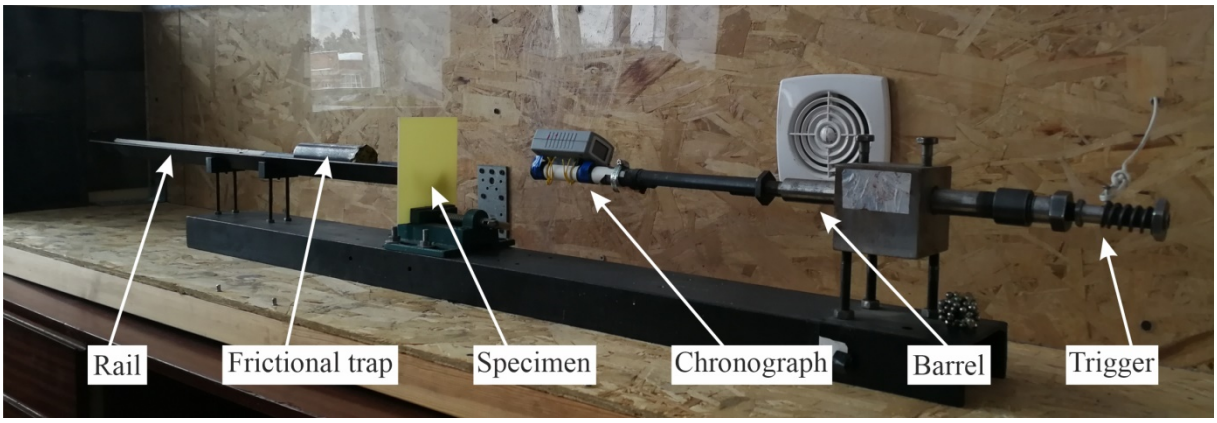


Fig. 2. The powder gun stand for ballistic tests

1. Material, specimens and methods

1.1. Material

Commercially available glass fibre-reinforced plastic «STEF» (JSC Elektroizolit) with a nominal thickness of 4 mm (4.1 ± 0.07) and 6 mm (6.1 ± 0.05 mm) based on a hot-curing epoxyphenol matrix was used as material for the research. Plain weave glass fabric (E-glass) was used as a reinforcement in the composite. The number of reinforcing filler layers in the composite was 20 and 30 for thicknesses of 4 and 6 mm, respectively. The material density was 1.77–1.79 g/cm^3. The fibre volume fraction in the material was determined by the burning method and was 42 % for both thicknesses. Tests were also carried out on specimens with a thickness of 7.3±0.05 mm, in which two types of glass fabric plain weave with different areal densities were used as reinforcement. The total number of reinforcement layers was 28. The material density was 1.83 g/cm^3 in this case, and the fibre volume fraction was 44 %. The elastic and strength characteristics of the material used in the research can be found in [29].

1.2. Ballistic tests procedure

A powder gun stand was used to perform ballistic tests [30] (fig. 2). Specimens with dimensions in the plane of 100 mm×140 mm (w×h) were cut from a large GFRP plate of corresponding thickness. A steel sphere with the diameter of 6.35 mm and the mass of 1.05 g was used as the projectile.

Standard mounting cartridges were used as the energy source. The initial projectile velocity was controlled by varying the amount of gunpowder in the cartridge.

The initial projectile velocity was determined at the barrel cut using an optical chronograph. To estimate the residual projectile velocity, a frictional trap with a weight of 665 g was used. Compacted aramid fabric was used as a filler to the frictional trap.

The projectile/trap interaction was considered absolutely inelastic. The coefficient of sliding friction f between the trap and the rail was determined experimentally and was 0.27. The residual projectile velocity was determined using a formula based on the laws of conservation of energy and momentum

$$V(S)=\left(1+\frac{M}{m_p}\right)\sqrt{2\,g\,f\,S}. \quad (1)$$

In formula (1) S is the sliding distance after the projectile and debris hit the trap, m_P is the projectile mass (including debris mass), M is the mass of the trap, and g is the acceleration of gravity.

The specimen prepared for testing was fixed on one side in a vice grip (Fig. 3). A shot was fired after installing the specimen.

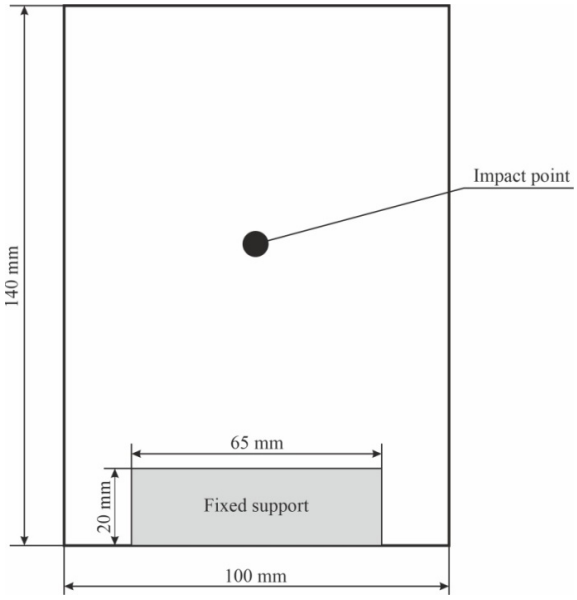


Fig. 3. Specimen fastening scheme

To approximate experimental points and obtain ballistic curves, the Lambert-Jonas equation was used [27]

$$V_r=\begin{cases}0 \text{ if } V_i<V_{50}\\ A(V_i^m-V_{50}^m)^{1/m} \text{ if } V_i\geq V_{50}\end{cases}, \quad (2)$$

where A, V_{50} and m are three regression parameters, V_r and V_i are residual and initial projectile velocities, respectively.

It was decided to perform ballistic tests in two stages. At the first stage, ballistic curves were obtained based on the test results of at least 20 specimens of each thickness using the Lambert – Jonas approximation. Initial estimates of V_{50} and the maximum perforation and non-perforation velocities were also obtained for GFRP specimens of three thicknesses. At the second stage, a series of tests was carried out for GFRP specimens of each thickness, in which the initial projectile velocity was selected so that it fell into the zone of mixed results to obtain perforation frequency curves.

1.3. Processing of results

To obtain a perforation probability curve (perforation frequency) near V_{50}, the result of the target/projectile interaction at various impact velocities was considered as a binary value U, where U=1 if perforation took place, and U=0 if no perforation occurred. Assuming that the initial projectile velocity near the ballistic limit was a random variable, and it followed the normal distribution law, the value of V_{50} for specimens of each thickness was determined as the arithmetic mean of the limit velocities V_0 and V_{100}. For the considered range of projectile velocities (ZMR), the value of V_{50} was also the mathematical expectation μ. The standard deviation (SD or σ), in this case, determined the zone of mixed results width.

To test the hypothesis about the normality of the initial projectile velocity distribution near V_{50}, the considered velocity range was divided into 7 intervals with a step of 3 m/s. At each interval, the relative probability of perforation/non-perforation was determined. It should be noted that it is necessary to relate the number of perforations to the number of shots fired in the ZMR in the V_0–V_{50} range, and the number of non-perforations to the number of tests in the ZMR in the V_{50}–V_{100} range. This action is explained by the fact that the value of V_{50} represents the velocity at which an equally probable outcome of the binary target/projectile interaction is possible. As the velocity shifts from V_{50} towards V_0, the probability of perforation decreases, and as it shifts towards V_{100}, the probability of non-perforation decreases. The hypothesis, that the random variable under consideration followed the normal distribution law, was tested using the χ^2 (Chi-square) goodness-of-fit criterion

$$\chi^2_{cr}=\chi^2_{cr}(\alpha,k);$$
$$\chi^2=\sum_{i=1}^{m}\frac{\left(n_i-n_i^{'}\right)^2}{n_i^{'}}; \quad (3)$$

where n_i are relative probabilities values of perforation/non-perforation obtained from the experiments;

$n_i^{'}$ are relative probabilities values of perforation/non-perforation obtained from the theoretical distribution;

α is significance level;

$k=m-r-1$ is degrees of freedom number of Chi-square distribution.

By integrating the probability density function, perforation probability curves for GFRP specimens near V_{50} were obtained.

2. Results and discussion

2.1. Ballistic curves

The values of parameters A, m and V_{50} (2) for each type of specimen were determined using the least squares method and are presented in Table 1. Figure 4 shows the obtained ballistic curves for each specimen thickness with actual test measurements plotted.

Table 1

Lambert – Jonas approximation parameters

Thickness, mm	A	m	V_{50}, m/s
4.0	0.825	2.171	280
6.0	0.893	1.962	399
7.3	0.843	1.893	465

The obtained estimates of the ballistic limit for the considered configuration of GFRP specimens with thicknesses of 4 mm, 6 mm and 7.3 mm were 280 m/s, 399 m/s and 465 m/s, respectively.

Figure 5 shows zones of mixed results (fragments of ballistic curves near V_{50}) for specimens of three thicknesses with the limit values of the initial projectile velocities plotted.

When determining the zone of mixed results width for GFRP specimens with a thickness of 4 mm, the maximum non-perforation velocity V_0 and the minimum perforation velocity V_{100} observed in the experiment were taken as the limit velocities V_0 and V_{100} as a first approximation. For specimens with a thickness of 6 mm, the maximum non-perforation velocity was taken as V_0, and the velocity of 403 m/s was taken as V_{100}, since at a lower velocity both perforation and non-perforation of the specimen were observed. Similarly, for specimens with a thickness of 7.3 mm, the maximum non-perforation velocity was taken as V_0, and the velocity of 486 m/s was chosen as V_{100}.

At the second stage of ballistic tests, the energy of the mounting cartridge was selected in such a way that the initial projectile velocity fell into the zone of mixed results. At least 70 tests were carried out for each thickness of GFRP specimens.

Based on the results of a new tests series, the estimation of V_{50} was refined, the width of the ZMR was adjusted, and new values of the velocities V_0 and V_{100} were obtained for specimens with a thickness of 4 mm. The refined V_{50} estimation was 275 m/s. The limit ZMR velocities V_0 and V_{100} were 271 m/s and 279 m/s, respectively (Fig. 6). The adjusted zone of mixed results width was 9 m/s.

2.2. Perforation stochasticity of 4 mm thick GFRP specimens

It should be noted that in the case of perforation, there was a significant scatter in the residual projectile velocities (up to ± 25 m/s) relative to the ballistic curve approximation. As the initial projectile velocity increased, the discrepancy between the experimental points and the approximation decreased. The observed scatter in the residual projectile velocities may be a consequence of the random nature of the material fracture on the specimen back side and the acceleration of the specimen debris.

It is also worth noting that constructing a perforation frequency curve with such a small ZMR width (less than 3% of the V_{50} value) is devoid of practical meaning. Shifting the permissible design velocity V_D [19] by 5 % of the V_{50} estimation eliminates the possibility of perforation.

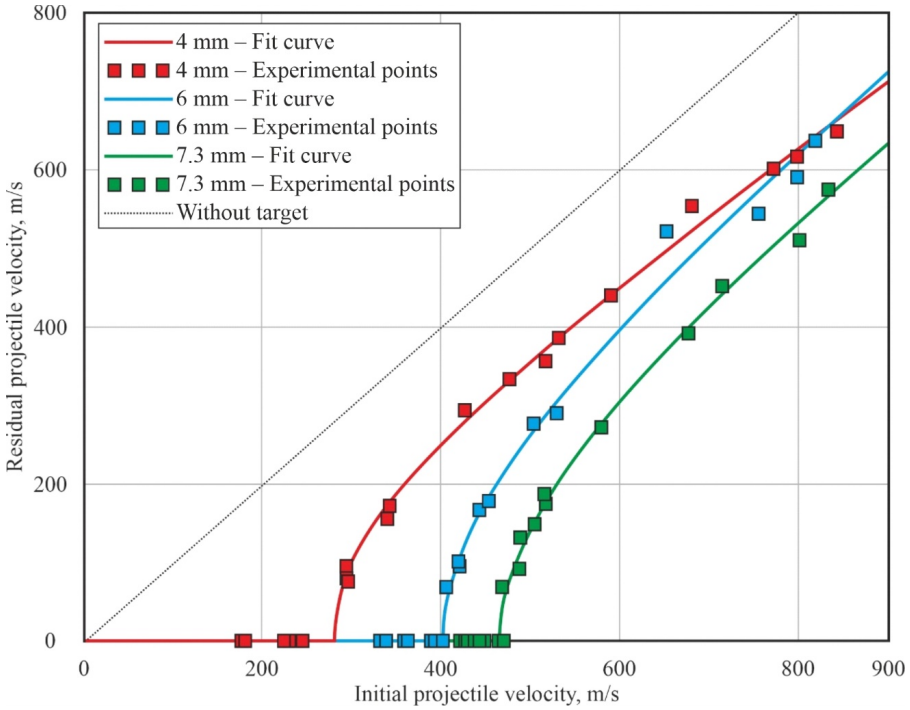


Fig. 4. Ballistic curves (Lambert – Jonas approximation) for GFRP specimens of three thicknesses

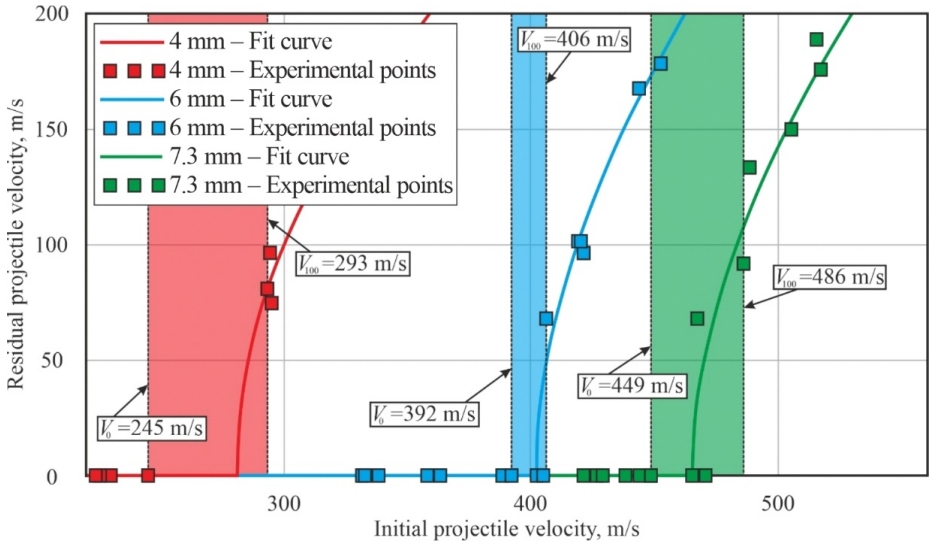


Fig. 5. Zones of mixed results for three thicknesses of GFRP specimens

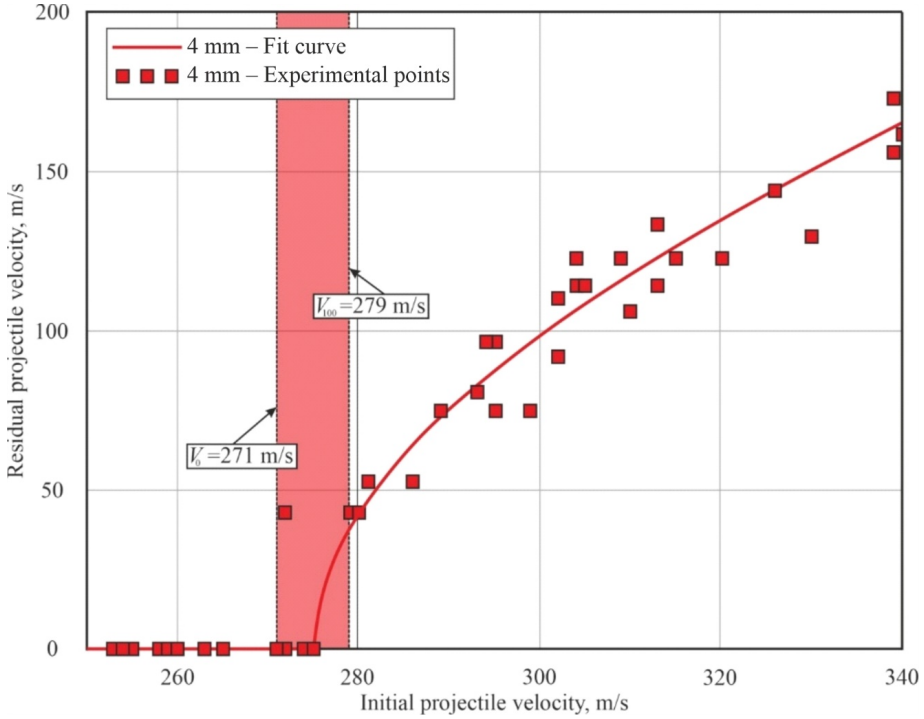


Fig. 6. Refined ZMR width for GFRP specimens with a thickness of 4 mm

Table 2

Refined values of V_{50} estimation and ZMR limit velocities

Thickness, mm	V_{50}, m/s	V_0, m/s	V_{100}, m/s	ZMR width, m/s
6.0	401	394	408	15
7.3	463	457	471	15

2.3. Perforation stochasticity of GFRP specimens with the thickness of 6 mm and 7.3 mm

For GFRP specimens with a thickness of 6 mm and 7.3 mm, the V_{50} estimations were also refined, the ZMR widths were adjusted, and new values of the velocities V_0 and V_{100} were obtained (Table 2). Figure 7 shows the fragments of ballistic curves in the vicinity of V_{50} with plotted limit ZMR velocities for GFRP specimens of two thicknesses.

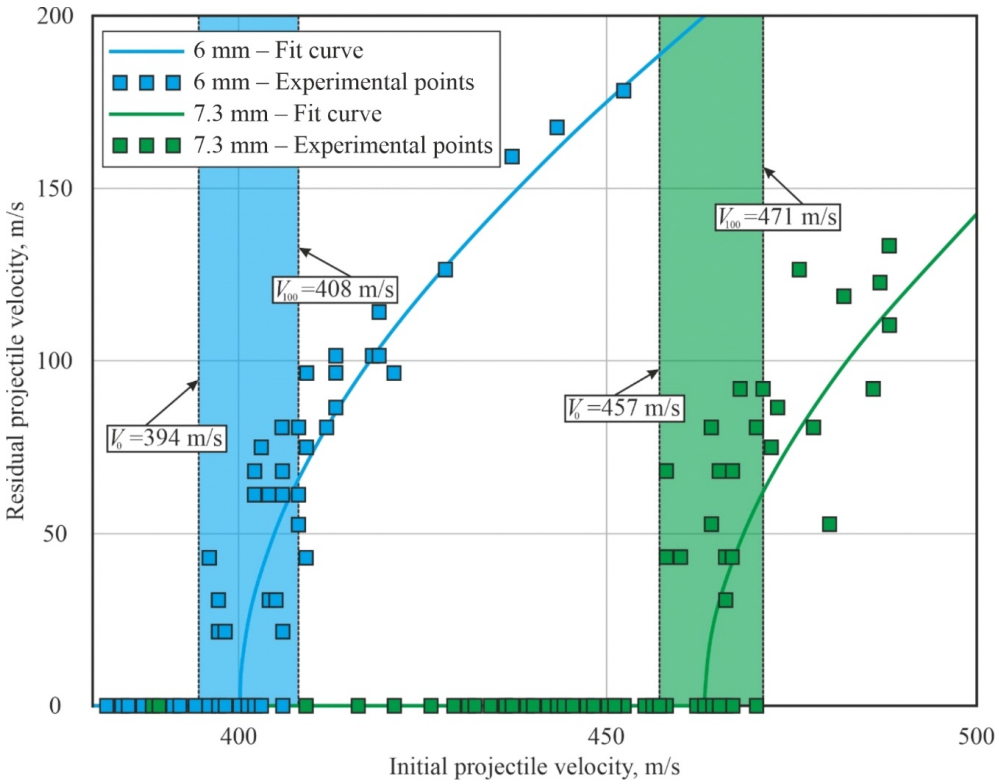


Fig. 7. Refined ZMR width for GFRP specimens with a thickness of 6 mm and 7.3 mm

The presented figure shows that as the target thickness increased, the scatter of the residual projectile velocity near V_{50} increased. For specimens with a thickness of 6 mm, a scatter of residual projectile velocities near V_{50} was up to ± 35 m/s, while for specimens with a thickness of 7.3 mm the scatter of residual projectile velocities was up to ± 60 m/s.

For the considered GFRP specimens of two thicknesses, the zone of mixed results width was 15 m/s. The ratio of the ZMR widths to the corresponding V_{50} values for specimens with nominal thicknesses of 6 mm and 7.3 mm did not exceed 4 %, which was significantly less than the scatter in the strength properties of the considered GFRP [29].

Figure 8 shows the results of the GFRP specimens 6 mm and 7.3 mm thick interaction with projectile at various impact velocities near the corresponding V_{50}.

Assuming that the initial projectile velocity near the ballistic limit was a random variable, and it followed the normal distribution law, the value of V_{50} for the specimens 6 mm thick was obtained as the arithmetic mean of the velocities V_0 and V_{100} and was 401 m/s. The mathematical expectation μ determined for the specimens with a thickness of 7.3 mm was 463 m/s. The standard deviation, in fact determining the width of ZMR, was 4.59 m/s and 4.62 m/s for GFRP specimens with actual thicknesses of 6 mm and 7.3 mm, respectively.

Figure 9 shows the calculated and experimental distribution density functions of a random variable for GFRP specimens of two thicknesses. The hypothesis that the random variable under consideration followed the normal distribution law was tested using the χ2 (Chi-square) goodness-of-fit criterion.

In accordance with (3)

$$\chi^2_{cr}(0,99;4) = 0,297;$$
$$\chi^2_{(6\text{ mm})} = 0,038 < \chi^2_{cr};$$
$$\chi^2_{(7,3\text{ mm})} = 0,113 < \chi^2_{cr}.$$

It was established that the variable under consideration followed the normal distribution law. Therefore, the probability (frequency) curve of GFRP specimens' perforation of two thicknesses can be described using normal probability distribution law.

Figure 10 shows the obtained perforation probability curves for GFRP specimens of two thicknesses with corresponding 2σ ranges.

The data on the ZMR width and perforation probability curve will be used in the future work dedicated to numerical analysis of GFRP perforation stochasticity under high-velocity impact. It is planned to conduct computational studies on the influence of material properties scatter on the energy absorption of the composite at impact velocities near the ballistic limit.

Conclusions

This paper presented the results of the experimental study on the steel sphere projectile interaction with GFRP specimens of three thicknesses at impact velocities near the corresponding ballistic limits, and the widths of the zones of

mixed results were obtained. For GFRP specimens with a thickness of 6 mm and 7.3 mm, the corresponding perforation probability curves were obtained using the normal distribution law. It was found that for GFRP specimens of three thicknesses considered, the ratio of the zone of mixed results width (in the 2σ range) to the corresponding V_{50} estimation was about 4 %. Thus, the scatter in determination of the maximum projectile velocity, corresponding to the zero probability of specimen perforation V_0, is less than the scatter of strength characteristics of GFRP specimens obtained during static tests. The data obtained can be used by engineers and designers to select a rational value for the safety factor when developing critical structures, as well as when planning similar experimental studies. Moreover, the width of zone of mixed results can be considered as a characteristic of the quality of material production.

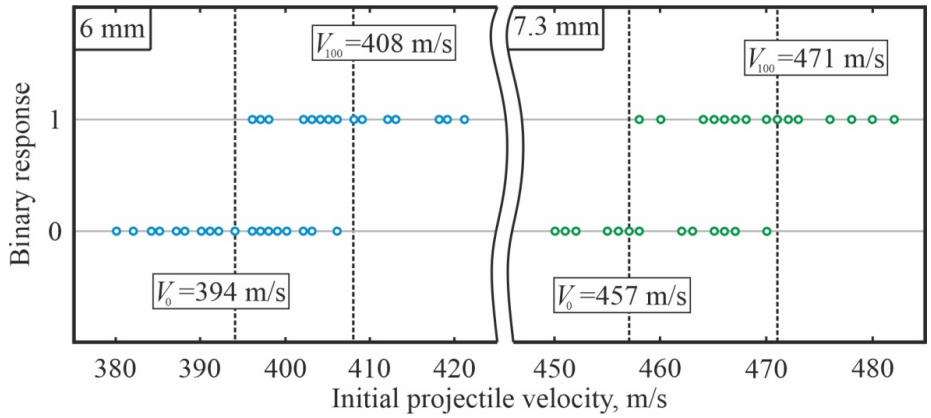


Fig. 8. Results of target/projectile interaction near the corresponding ballistic limit for specimens of two thicknesses

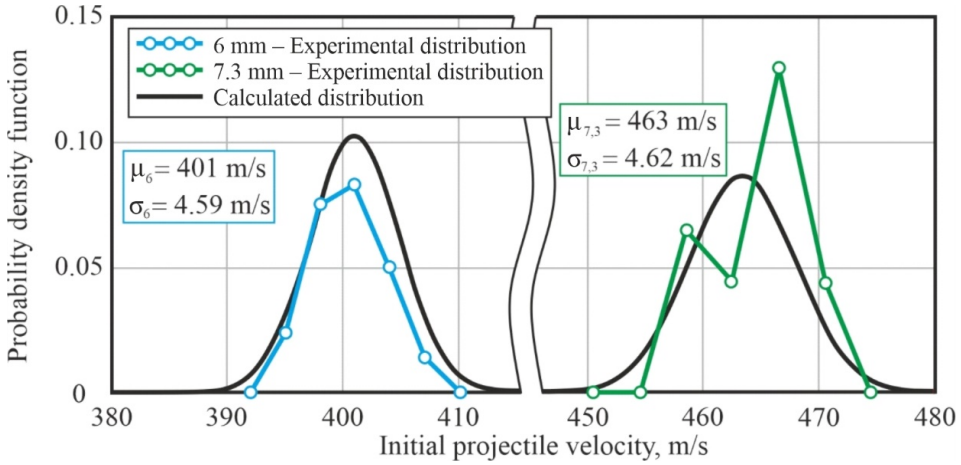


Fig. 9. Experimental and calculated probability density functions for GFRP specimens of two thicknesses

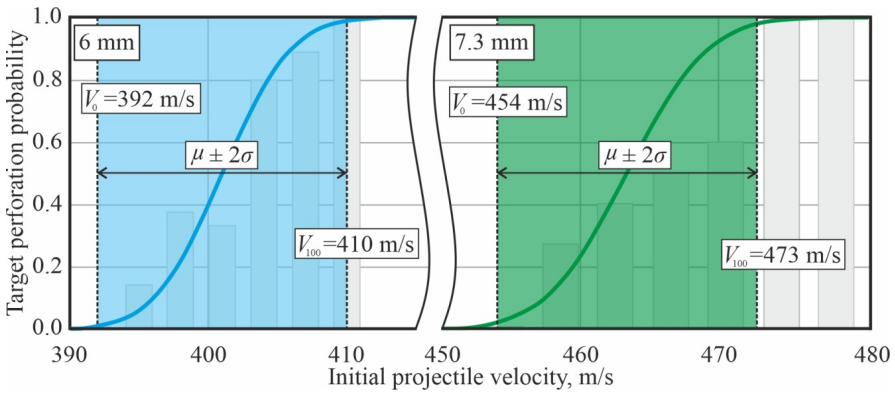


Fig. 10. Perforation probability curves near V_{50} for GFRP specimens of two thicknesses

References

1. Bouvet C., Rivallant, S. Damage tolerance of composite structures under low-velocity impact. In: Dynamic Deformation, Damage and Fracture in Composite Materials and Structures, Silberschmidt V.V. (Eds). Woodhead Publishing, Elsevier, Cambridge, 2016, pp. 7-33. DOI: 10.1016/b978-0-08-100080-9.00002-6

2. Verma A.S., Yan J., Hu W., Jiang Z., Shi W., Teuwen, J. J. E. A review of impact loads on composite wind turbine blades: Impact threats and classification. *Renewable and Sustainable Energy Reviews*, 2023, Vol. 178, 113261. DOI: 10.1016/j.rser.2023.113261

3. Sutherland L. S. A review of impact testing on marine composite materials: Part I – Marine impacts on marine composites. *Composite Structures*, 2018, Vol. 188, pp. 197–208. DOI: 10.1016/j.compstruct.2017.12.073

4. Mraih H., Hashemi J., Kalfat R., Al-Mahaidi R., Lu G. Comparative Assessment of FRP Composite Materials in Structural Applications under Low-Velocity Impact Loads: A Review. *Procedia Structural Integrity*, 2024, Vol. 64, pp. 1402-1410. DOI: 10.1016/j.prostr.2024.09.380

5. Kurteyev V.A., Burdyugov S.I., Inozemtsev A.A., Lomaev V.I., Mozerov B.G., Sokolovskiy M.I., Shatrov, V.B. Strength computational and experimental analysis of turbojet fan case under the impact of a torn blade. *PNRPU Mechanics Bulletin*, 2017, No. 1, pp. 85–103. DOI: 10.15593/perm.mech/2017.1.06

6. Yu G., Li X., Huang W. Performance and Damage Study of Composite Rotor Blades under Impact. *Polymers*, 2024, Vol. 16, 623. DOI: 10.3390/polym16050623

7. Tsirogiannis E.Ch., Daskalakis E., Vogiatzis C., Psarommatis F., Bartolo P. Advanced composite armor protection systems for military vehicles: Design methodology, ballistic testing, and comparison. *Composites Science and Technology*, 2024, Vol. 251, 110486. DOI: 10.1016/j.compscitech.2024.110486

8. Wang K., Taheri F. A comparative investigation into the high-velocity impact (HVI) and compression after impact (CAI) responses of a novel 3d hybrid composite and carbon and glass fiber-reinforced composites. *Composites Part B: Engineering*, 2025, Vol. 292, 112075. DOI: 10.1016/j.compositesb.2024.112075

9. Phadnis V.A., Roy A., Silberschmidt V.V. Dynamic damage in FRPs: From low to high velocity. In: Dynamic Deformation, Damage and Fracture in Composite Materials and Structures (Second Edition), Silberschmidt V.V. (Eds). Woodhead Publishing, Elsevier, Cambridge, 2023, pp. 165-193. DOI: 10.1016/B978-0-12-823979-7.00008-9

10. Li N., Du J., Lee H.M., Liu W., Zheng Y., Lee H.P. Damage characterization and modelling of FRP laminated composites subjected to external edge-on impact. *Composites Part B*, 2024, Vol. 287, 111879. DOI: 10.1016/j.compositesb.2024.111879

11. Mouritz A.P. Advances in understanding the response of fibre-based polymer composites to shock waves and explosive blasts. *Composites Part A: Applied Science and Manufacturing*, 2019, Vol. 125, 105502. DOI: 10.1016/j.compositesa.2019.105502

12. Andrew J.J., Srinivasan S.M., Arockiarajan A., Dhakal H.N. Parameters influencing the impact response of fiber-reinforced polymer matrix composite materials: A critical review. *Composite Structures*, 2019, Vol. 224, 111007. DOI: 10.1016/j.compstruct.2019.111007

13. Impact Engineering of Composite Structures, Abrate S. (Eds). Springer Vienna, 2011, 403 p. DOI: 10.1007/978-3-7091-0523-8

14. Sutherland L.S. A review of impact testing on marine composite materials: Part II – Impact event and material parameters. *Composite Structures*, 2018, Vol. 188, pp. 503-511. DOI: 10.1016/j.compstruct.2018.01.041

15. Sutherland L.S. A review of impact testing on marine composite materials: Part III – Damage tolerance and durability. *Composite Structures*, 2018, Vol. 188, pp. 512–518. DOI: 10.1016/j.compstruct.2018.01.042

16. Davies G.A.O., Olsson R. Impact on composite structures. *The Aeronautical Journal*, 2004, Vol. 108, No. 1089, pp. 541–563. DOI: 10.1017/S0001924000000385

17. Tahenti B., Coghe F., Nasri R. Ballistic Limit Estimation Approaches for Ballistic Resistance Assessment. *Defence Science Journal*, 2020, Vol. 70, No. 1, pp. 82-89. DOI: 10.14429/dsj.70.14122

18. Johnson T.H., Freeman L., Hester J., Bell J.L. Comparison of ballistic resistance testing techniques in the Department of Defense. *IEEE Access*, 2014, Vol. 2, pp. 1442-1455. DOI: 10.1109/ACCESS.2014.2377633

19. Crouch I. Introduction to armour materials. In: The science of armour materials, 1st Edition, Crouch I. (Eds). Woodhead Publishing. Elsevier, 2017, pp. 1-54. DOI: 10.1016/B978-0-08-100704-4.00001-3

20. Reddy P.R.S., Savio S. G, Madhu V. Ceramic Composite Armour for Ballistic Protection. In: Handbook of Advanced Ceramics and Composites. Mahajan Y. and Roy J. (Eds). Springer International Publishing, 2020, pp. 1-46. DOI: 10.1007/978-3-319-73255-8_10-1

21. Dixon W.J. Mood A.M. A method for obtaining and analyzing sensitivity data. *Journal of the American Statistical Association*, 1948, Vol. 43, No 241, pp. 109-126. DOI: 10.1080/01621459.1948.10483254

22. Joseph V.R. Efficient Robbins-Monro Procedure for Binary Data. *Biometrika*, 2004, Vol. 91, No 2, pp. 461-467. DOI: 10.1093/biomet/91.2.461

23. Talbott D.V. Approaches to implementing deterministic models in a probabilistic framework. JSME Pressure Vessels and Piping Conference. Honolulu, Hawaii, 1995.

24. Mauchant D., Rice K.D., Riley M.A., Lebber D., Samarov D., Forster A.L. Analysis of Three Different Regression Models to Estimate the Ballistic Performance of New and Environmentally Conditioned Body Armor. National Institute of Standards and Technology, 2011. DOI: 10.6028/NIST.IR.7760

25. Tahenti B., Coghe F., Nasri R., Pirlot M. Armor's Ballistic Resistance Simulation Using Stochastic Process Modeling, *International Journal of Impact Engineering*, 2017, Vol. 102, pp. 140-146. DOI: 10.1016/j.ijimpeng.2016.12.009

26. Neyer B.T. A D-Optimality-Based Sensitivity Test. *Technometrics*, 1994, V. 36, No 1, pp. 61-70. DOI: 10.2307/1269199

27. Lambert J.P. Jonas G.H. Towards standardization in terminal ballistics testing: Velocity representation: BRL Report No. 1852. U.S. Army Ballistic Research Laboratories. – MD.: Aberdeen Proving Ground, 1976, p. 51.

28. Kudryavtsev O. A., Zhikharev M. V., Olivenko N. A. Creation and verification of computational models for analysis of the mechanical behaviour of jet engines composite components under high-velocity impact: Main problems and basic recommendations. *PNRPU Mechanics Bulletin*, 2019, No. 4, pp. 68–79. DOI: 10.15593/PERM.MECH/2019.4.07

29. Kudryavtsev O. A., Ignatova A. V., Olivenko N. A. The influence of thickness on residual flexural strength of composite with low-velocity impact damages: experimental study. *PNRPU Mechanics Bulletin*, 2021, No. 3, pp. 6-11. DOI: 10.15593/perm.mech/2021.3.01

30. Sapozhnikov S.B. Kudryavtsev O.A. Kompaktnyi razgonnyi stend dlia ballisticheskikh ispytaniy [Compact accelerator for ballistic testing]. *Bulletin of the South Ural State University. Series "Mechanical Engineering Industry"*, 2012, Vol. 20, No. 33, pp. 139-143.

Funding. The study was not supported by sponsorship.
Conflict of interest. The authors declare no conflict of interest.
The contribution of the authors is equivalent.

Финансирование. Исследование не имело спонсорской поддержки.
Конфликт интересов. Авторы заявляют об отсутствии конфликта интересов.
Вклад авторов равноценен.